Supplemental Material

Path integral Monte Carlo determination of the fourth-order virial coefficient for unitary two-component Fermi gas with zero-range interactions

Yangqian Yan[1] and D. Blume[1]

[1]*Department of Physics and Astronomy, Washington State University, Pullman, Washington 99164-2814, USA*

The notation employed in this Supplemental Material follows that introduced in the main text.

I. LITERATURE VALUES OF b_4

Table S1 summarizes the literature results for the fourth-order virial coefficient; this table is an extended version of Table I of the main text. The non-interacting contribution to the total fourth-order virial coefficient $b_4^{\mathrm{hom,tot}}$ of the homogeneous system is given by

$$b_n^{\mathrm{hom,ni}} = (-1)^{n+1}/n^{5/2};\qquad\qquad(\mathrm{S1})$$

the interacting part of the fourth-order virial coefficient b_4^{hom} of the homogeneous system is defined through

$$b_n^{\mathrm{hom}} = b_n^{\mathrm{hom,tot}} - b_n^{\mathrm{hom,ni}}.\qquad\qquad(\mathrm{S2})$$

TABLE S1: Summary of literature results. The value reported in the respective reference is underlined. The conversion to other "representations" is done using Eqs. (S1)-(S3). The column labeled "Ref." refers to the bibliography of the main text.

b_4^{hom}	$b_4^{\mathrm{hom,tot}}$	b_4^0	Ref.	comment
<u>0.096(15)</u>	0.065(15)	0.01200(188)	19	ENS experiment
0.096(10)	<u>0.065(10)</u>	0.01203(125)	26	MIT experiment
-0.016(4)	-0.04725(40)	<u>-0.0020(5)</u>	22	sum-over-states approach
<u>0.06</u>	0.02875	0.0075	23	diagrammatic approach
-0.063(1)	-0.09425(10)	-0.007875(125)	24	3-body inspired conjecture

The interacting part of the fourth-order virial coefficient b_4^0 of the harmonically trapped system at high temperature and b_4^{hom} are related via (see also the main text),

$$b_n^{\text{hom}} = n^{3/2} b_n^0. \tag{S3}$$

II. PAIR PRODUCT APPROXIMATION AND ZERO-RANGE DENSITY MATRIX

Equation (9) of the main text writes the observable $Q_{n_1,n_2}^{\text{ni}}/Q_{n_1,n_2}$ in terms of the density matrices $\rho^{\text{ni}}(\mathbf{R}_i, \mathbf{R}_{i+1}; \tau)$ and $\rho(\mathbf{R}_i, \mathbf{R}_{i+1}; \tau)$ of the non-interacting and unitary (n_1, n_2)-particle systems. To evaluate the density matrix by the PIMC approach, we use the pair product approximation [1],

$$\rho(\mathbf{R}, \mathbf{R}'; \tau) \approx \left(\prod_{j=1}^{n_1+n_2} \rho^{\text{sp}}(\mathbf{r}_j, \mathbf{r}'_j; \tau) \right) \times$$
$$\left(\prod_{j=1}^{n_1} \prod_{k=n_1+1}^{n_1+n_2} \bar{\rho}^{\text{rel}}(\mathbf{r}_j - \mathbf{r}_k, \mathbf{r}'_j - \mathbf{r}'_k; \tau) \right), \tag{S4}$$

where $\rho^{\text{sp}}(\mathbf{r}, \mathbf{r}'; \tau)$ is the single-particle density matrix [1],

$$\rho^{\text{sp}}(\mathbf{r}, \mathbf{r}'; \tau) = a_{\text{ho}}^{-3} \left[2\pi \sinh(\tau\hbar\omega) \right]^{-3/2} \times$$
$$\exp\left(-\frac{(\mathbf{r}^2 + \mathbf{r}'^2)\cosh(\tau\hbar\omega) - 2\mathbf{r}\cdot\mathbf{r}'}{2\sinh(\tau\hbar\omega)a_{\text{ho}}^2} \right), \tag{S5}$$

and $\bar{\rho}^{\text{rel}}(\mathbf{r}, \mathbf{r}'; \tau)$ is the reduced pair density matrix of the relative two-body problem with zero-range interaction [2],

$$\bar{\rho}^{\text{rel}}(\mathbf{r}, \mathbf{r}'; \tau) = 1 + \frac{2\hbar^2\tau}{mrr'} \exp\left(-\frac{m(rr' + \mathbf{r}\cdot\mathbf{r}')}{2\hbar^2\tau} \right). \tag{S6}$$

The density matrix ρ^{ni} of the non-interacting system is given by Eq. (S4) with $\bar{\rho}^{\text{rel}}$ replaced by 1.

III. EXTRAPOLATION TO THE $\tau \to 0$ LIMIT AND SELECTED RAW DATA

As mentioned in the main text, to determine b_n with comparable percentage accuracy at all temperatures, $Q_{n_1,n_2}^{\text{ni}}/Q_{n_1,n_2}$ has to be determined with increasing percentage accuracy with increasing temperature. To ensure that our results are free of systematic errors, the error introduced by the $\tau \to 0$ extrapolation has to be smaller than the error of the extrapolation that arises from the statistical error of the individual PIMC data points. To illustrate this, we consider the (2,1) system at the highest temperature considered, i.e., at $k_B T = 2E_{\text{ho}}$.

Circles in Fig. S1(a) show $Q_{2,1}^{\text{ni}}/Q_{2,1}$, obtained by our PIMC approach, as a function of the imaginary time step τ (the data correspond to $N = 2, 3, 4$, and 6). The solid line shows a fourth-order fit of the form $a + b\tau^2 + c\tau^4$ to our
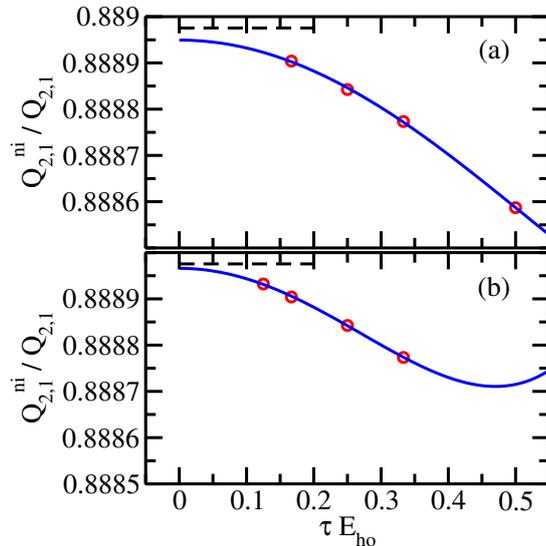
FIG. S1: (Color online) Benchmarking our PIMC results (circles) for the (2,1) system at unitarity through comparison with sum-over-states results. The observable $Q_{2,1}^{\mathrm{ni}}/Q_{2,1}$ as a function of the imaginary time step τ at temperature $k_B T = 2E_{\mathrm{ho}}$. The error bars (not shown) are smaller than the symbol size. In (a), the time steps correspond to $N = 2, 3, 4$, and 6. In (b), the time steps correspond to $N = 3, 4, 6$, and 8. The solid line shows the fourth-order polynomial fit of the form $a + b\tau^2 + c\tau^4$. The dashed line shows the sum-over-states results.

PIMC data. The extrapolated $\tau \to 0$ value of 0.888949(8), where the error bar accounts for the statistical uncertainty of the PIMC data, deviates by about 3 standard deviations (or 0.003%) from the sum-over-states result of 0.8889755. We attribute the discrepancy to the fact that the τ considered are not small enough for the fourth-order fit to be fully reliable. To corroborate this interpretation, we (i) employ a sixth-order fit and (ii) apply the fourth-order fit to PIMC data for smaller τ. The sixth-order fit (using, as before, the data corresponding to $N = 2, 3, 4$, and 6) yields 0.888964(19), in agreement with the sum-over-states result. Note, however, that the error bar is much larger than that resulting from the fourth-order fit; the reason is that we are attempting to determine four fit parameters using just four data points. Performing a fourth-order fit to the PIMC data for $N = 3, 4, 6$, and 8 yields 0.888966(8), which almost agrees with the sum-over-states approach within error bar and with an error bar that is comparable to our previous fourth-order fit [see Fig. S1(b)]. This analysis suggests that our PIMC calculations are free of systematic errors provided we go to sufficiently small τ.

Table S2 lists the PIMC raw data for the (3,1) and (2,2) systems at various temperatures (the data for low temperatures are not shown). We report the observables $Q_{3,1}^{\mathrm{ni}}/Q_{3,1}$ and $Q_{2,2}^{\mathrm{ni}}/Q_{2,2}$ for various time slices. For $E_{\mathrm{ho}}/(k_B T) = 0.6, 0.7$, and 0.8, the largest number of time slices considered is $N_{\max} = 9$. For $E_{\mathrm{ho}}/(k_B T) = 0.5$, our

TABLE S2: Selected PIMC raw data. Columns 1 and 2 show the inverse temperature $E_{\mathrm{ho}}/(k_B T)$ and the number of imaginary time slices N, respectively. Columns 3 and 4 show the observables $Q_{3,1}^{\mathrm{ni}}/Q_{3,1}$ and $Q_{2,2}^{\mathrm{ni}}/Q_{2,2}$ for the (3,1) and (2,2) systems, respectively.

$E_{\mathrm{ho}}/(k_B T)$	N	$Q_{3,1}^{\mathrm{ni}}/Q_{3,1}$	$Q_{2,2}^{\mathrm{ni}}/Q_{2,2}$
0.5	2	0.8413081(35)	0.7940517(46)
0.5	3	0.8418155(43)	0.7946990(43)
0.5	4	0.8420157(41)	0.7949482(45)
0.5	6	0.8421806(41)	0.7951732(53)
0.6	3	0.754475(16)	0.686274(11)
0.6	4	0.754955(12)	0.686860(11)
0.6	5	0.755218(12)	0.687174(14)
0.6	7	0.755450(13)	0.687445(14)
0.6	9	0.755591(15)	0.687587(14)
0.7	3	0.658547(24)	0.571429(24)
0.7	4	0.659464(22)	0.572473(14)
0.7	6	0.660203(26)	0.573329(22)
0.7	9	0.660583(29)	0.573764(23)
0.8	4	0.563935(34)	0.462752(36)
0.8	5	0.564662(35)	0.463530(33)
0.8	7	0.565379(36)	0.464433(32)
0.8	9	0.565708(38)	0.464757(33)

available computing resources limit us to $N_{\max} = 6$, resulting in reduced accuracy of the observables.

For $E_{\mathrm{ho}}/(k_B T) = 0.6$, 0.7, and 0.8, we perform fourth-order fits to the τ-dependent $Q_{3,1}^{\mathrm{ni}}/Q_{3,1}$ and $Q_{2,2}^{\mathrm{ni}}/Q_{2,2}$ data listed in Table S2, yielding extrapolated $\tau \to 0$ values with error bars between 0.0024% and 0.016%. We estimate, based on our tests for the three-body system, that these statistical errors are larger than the systematic error, which arises from the use of the fourth-order fit. Hence the systematic uncertainty can be neglected. For $E_{\mathrm{ho}}/(k_B T) = 0.5$, a fourth-order fit to the data given in Table S2 yields error bars of 0.0008% and 0.001% for $Q_{3,1}^{\mathrm{ni}}/Q_{3,1}$ and $Q_{2,2}^{\mathrm{ni}}/Q_{2,2}$, respectively. Since we estimate the systematic fit uncertainty to be, based on our analysis for the (2,1) system, about 0.003%, we deem the fourth-order fit unreliable. Using a sixth-order fit (which yields a larger error bar), we find the

TABLE S3: Selected extrapolated PIMC results. Columns 1 and 2 show the inverse temperature $E_{\mathrm{ho}}/(k_B T)$ and the order used in the extrapolation, respectively. Columns 3 and 5 show the extrapolated $\tau \to 0$ observables $Q_{3,1}^{\mathrm{ni}}/Q_{3,1}$ and $Q_{2,2}^{\mathrm{ni}}/Q_{2,2}$ for the (3,1) and (2,2) systems, respectively. Columns 4 and 6 show the resulting subcluster contributions $b_{3,1}$ and $b_{2,2}/2$, respectively, to the fourth-order virial coefficient.

$E_{\mathrm{ho}}/(k_B T)$	order	$Q_{3,1}^{\mathrm{ni}}/Q_{3,1}$	$b_{3,1}$	$Q_{2,2}^{\mathrm{ni}}/Q_{2,2}$	$b_{2,2}/2$
0.5	6	0.842330(15)	0.0194(16)	0.795393(18)	$-0.0139(16)$
0.6	4	0.755751(18)	0.0153(4)	0.687775(18)	$-0.0102(4)$
0.7	4	0.660877(39)	0.0135(3)	0.574108(30)	$-0.0095(2)$
0.8	4	0.566227(82)	0.0111(2)	0.465415(73)	$-0.0093(2)$

values listed in Table S3.

[1] D. M. Ceperley, "Path integrals in the theory of condensed helium," Rev. Mod. Phys. **67**, 279 (1995).

[2] Y. Yan and D. Blume, "Incorporating exact two-body propagators for zero-range interactions into N-body Monte Carlo simulations," Phys. Rev. A **91**, 043607 (2015).